MATCH
Communications in Mathematical and in Computer Chemistry

MATCH Commun. Math. Comput. Chem. **71** (2014) 47-56

ISSN 0340 - 6253

Average Deactivation Time of the Heterogeneous Reaction $2A + B_2 \longrightarrow 2AB$

V. E. Pastor[1], P. L. Dammig Quiña[1], L. M. Salvatierra[1,2], I. M. Irurzun[1], E. E. Mola[1,2,*]

[1] *CCT La Plata-CONICET, Instituto Nacional de Investigaciones Fisicoquímicas Teóricas y Aplicadas (INIFTA), Facultad de Ciencias Exactas, Universidad Nacional de La Plata, Diagonal 113 y Calle 64, CP 1900 La Plata, Argentina*

[2] *Facultad de Química e Ingeniería, Pontificia Universidad Católica Argentina, Mendoza 4197, CP 2000 Rosario, Argentina*

(Received April 15, 2013)

Abstract

In the present paper we exactly solve the distributed parameter stochastic model of the heterogeneous catalytic reaction $2A + B_2 \rightarrow 2AB$ and calculate the average number of reactive steps necessary to deactivate the lattice first,$< t >$. Results are compared with Monte Carlo simulations. $< t >$ shows a nonmonotonic behavior with the sticking coefficient probability s and the desorption probability p_d, reaching a maximum value that depends on s, p_d and the lattice size N.

1 Introduction

The understanding of the kinetics of heterogeneous catalytic reactions on small metal particles is of both theoretical and practical importance [1–4]. Real catalysts usually consist of small metal particles (1–20 nm) deposited on the internal surface of an inactive

*eemola@inifta.unlp.edu.ar

porous support and there are simulations describing the kinetics of heterogeneous catalytic reactions in nanosized domains [5,6].

In recent years we have made a considerable effort to develop analytical methods to find exact solutions in small domains to different problems dealing with (i) the kinetics of immobile adsorption of linear molecules on a two-dimensional lattice [7]; (ii) the average number of adsorption attempts (normalized by the number of adsorption sites) required for monolayer formation [8]; (iii) the branch counting probability approach to random sequential adsorption [9]; (iv) the scaling properties in the average number of attempts until saturation in random sequential adsorption processes [10]; (v) a heterogeneous reaction exactly solved on a small lattice [11]; (vi) the configurational degeneracy of a set of dipoles in a quasi-two-dimensional system [12].

In [11] we considered a generic bimolecular reaction over a single-crystal catalyst

$$2A + B_2 \rightarrow 2AB \tag{1}$$

that was designated the AB_2 model.

Here we consider this model, which includes the adsorption and desorption steps of reactants A and B_2, surface reaction between adsorbed species, and desorption of product AB (see *Eqs 2– 6*).

In the present article the AB_2 model is exactly solved on a small lattice and the *Average Deactivation Time* $< t >$ is calculated. $< t >$ is the average number of reactive steps necessary to deactivate the lattice first.

We show that the general behavior exhibited by this analytical solution in small domains is the same as the one observed in Monte Carlo simulations on larger surfaces. So finding analytical solutions to kinetic reaction mechanisms is useful prior to performing time-consuming computational simulations.

The paper is organized as follows: in Section 2, the model reaction is presented; in Section 3 results are compared with Monte Carlo simulations, and then conclusions are summarized.

2 The Model

The heterogeneous reaction model proceeds through the mechanism

$$A_{(g)} + * \longrightarrow A^* \qquad k_a, s \tag{2}$$

$$A^* \longrightarrow A_{(g)} + * \qquad k_d \tag{3}$$

$$B_{2(g)} + 2* \longrightarrow 2B^* \qquad k_a, s \tag{4}$$

$$B^* + B^* \longrightarrow B_{2(g)} + 2* \qquad k_d \tag{5}$$

$$A^* + B^* \longrightarrow AB_{(g)} + 2* \qquad k_r \tag{6}$$

where k_a, k_d and k_r are the rate constants for adsorption, desorption and reaction, respectively, $*$ denotes a vacant site on the catalyst surface, and s stands for the sticking coefficient probability. The subindex (g) represents a molecule in the gaseous phase, and a superindex $*$ stands for adsorbed species. A molecules require single adsorption sites in order to be adsorbed (see *Eq.2*). B_2 molecules must be chemisorbed with dissociation. This process requires two neighboring lattice sites (see *Eq.4*) and is involved in a number of surface reactions such as $CO + O_2$ and $NO + NH_3$ on $Pt100$**.** The reaction step, *Eq. 6,* requires the existence of two neighboring sites occupied by different adsorbates. The desorption of B_2 molecules is a second-order process and requires the existence of two neighboring lattice sites occupied by B^* adsorbates. We have considered first-nearest neighbors in both analytical calculations and Monte Carlo simulations.

In the adsorption steps, *Eqs. 2* and *4*, k_a is the impingement rate of the molecules and s is the sticking coefficient, which is the probability of a molecule to be adsorbed after the first impact on an adsorption site [13]. If the sticking coefficient is less than 1 ($s < 1$), there will be the possibility of finding microstates with empty sites. The desorption steps, *Eqs. 3* and *5,* and the reaction step, *Eq. 6,* are controlled by rate equations k_d and k_r.

The desorption probability p_d is one of the adjustable parameters in our model. The desorption probability p_d defines the relative rates of desorption to surface reaction.

$$p_d = \frac{k_d}{k_r + k_d} \tag{7}$$

Equal k_d values were assumed for both species. Although this is not the most general situation, it provides a simple illustration of the analytical method developed. Considering different rates of desorption involves introducing an additional adjustable parameter, i.e., the transition probabilities between microstates will depend on three variables.

The second adjustable parameter in our model is the sticking coefficient s (variations of k_a are usually included in s variations). Equal initial partial pressures of the reactants have been assumed to decrease the number of adjustable parameters to be used. Relative partial pressures of the reactants satisfy $p_A + p_{B_2} = 1$. Different initial partial pressure values can be considered in the model by introducing a factor p_A (or p_{B_2}) multiplying the sticking coefficient s, to calculate the transition probabilities between those microstates involving adsorption of A (or B_2) molecules. In many experiments the ratio p_A/p_{B_2} is maintained constant and then the above situation implies to use two different sticking coefficients (s_A and s_{B_2}), i.e., the transition probabilities between microstates will depend again on three variables.

In this article we aim to analyze whether an exact analytical solution in small domains may predict the general aspects of the solutions in larger domains.

For simplicity reasons, a limited range of situations has been considered. Diffusion processes of absorbed species have not been included either. In many real situations, the mobility of at least one of the reactants is fast. This fact may be included in the model by replacing the absolute certainty of whether one species (the mobile one) will be present or not in a neighboring site with an average value inversely proportional to the species mobility.

Both s and p_d vary from 0 to 1, and a comparison with the experiment has been given [11]. As an example, in the CO + O_2 reaction on $Pt100$ experimental values of $k_a = 2.22 \times 10^5 mbar^{-1}s^{-1}$ (for CO), $k_d = 40s^{-1}$ (for CO) and $k_r = 324s^{-1}$ have been given at $T = 500K$. These rate constant values determine p_d values of 0.11. For both CO and O_2 on $Pt100$, values of $s = 0.89$ and 0.28, respectively, have been reported at low coverages [13].

A square 2×2 lattice was used to represent the catalytic surface. This surface was assumed to be uniform, periodic boundary conditions were imposed and first nearest neighbors were considered. With these conditions there are 21 (twenty-one) different microstates (see *Fig.* 1) that can be observed with degeneracies $g_1 = 2, g_2 = 4, g_3 = 4, g_4 = 4, g_5 = 1$, $g_6 = 1, g_7 = 4, g_8 = 8, g_9 = 4, g_{10} = 4, g_{11} = 8, g_{12} = 4, g_{13} = 4, g_{14} = 8, g_{15} = 4, g_{16} = 2, g_{17} = 4, g_{18} = 2, g_{19} = 4, g_{20} = 4$, and $g_{21} = 1$. By choosing equal values of partial pressure for reactants A and B_2 ($p_A = p_{B_2} = 0.5$), the probability p_i of a macroscopic state was given by $p_i = g_i/81$. The origin of normalization factor 81 is

due to the fact that we have three different options to place in each lattice site, therefore $81 = 3^4$.

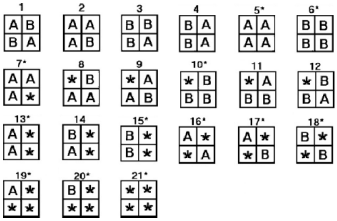

Figure 1: The 21 different microstates that can be observed in our model on a 2×2 square lattice with periodic boundary conditions.

There is a probability P_{ij} for the transition from state i to j. All these transition probabilities can be collected in a 21×21 matrix, e.g. the non zero matrix elements of the 11^{th} row of the matrix (see *Fig.* 2) are: $P_{11,4} = \frac{1}{4}s(1 + \frac{1}{2}p_d)$, $P_{11,6} = \frac{1}{8}sp_d$, $P_{11,7} = \frac{1}{4}sp_d$, $P_{11,8} = \frac{1}{4}s(1 - p_d)$, $P_{11,10} = \frac{1}{4}s(1 - p_d)$, $P_{11,11} = \frac{1}{4}(2 + sp_d - s - p_d)$, $P_{11,15} = \frac{1}{4}p_d(1 - s)$, $P_{11,19} = \frac{1}{2}p_d(1 - s)$, $P_{11,20} = \frac{1}{2}(1 - p_d)(1 - s)$.

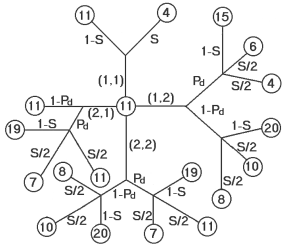

Figure 2: The transition probabilities starting from microstate 11 (see *Fig.* 1).

In an analogous way, the nonzero matrix elements of the remaining twenty rows of the probability matrix can be derived.

Let e_{ik} be the probability of arriving first at microstate i in k steps, therefore if $k = 0$,

$$e_{i0} = p_i, \qquad i = 1, 2, ..., 21 \tag{8}$$

if $k > 0$,

$$e_{ik} = \sum_j e_{jk-1} P_{ji} \tag{9}$$

where the summation is restricted to reactive microstates, i.e., those identified without asterisk in *Fig. 1*, whereas i runs all over the microstates shown in *Fig 1*, $i = 1, 2, 3, ...21$.

P_{ji} stands for the transition probability from state j to i as defined above. The summation is restricted because we are interested in knowing the average deactivating time $< t >$, i.e., we are evaluating the probability of arriving at microstate i in k steps without previously visiting a nonreactive microstate. We are also interested in knowing how $< t >$ depends on p_d and s.

Let $U(k)$ be the probability of arriving first at a nonreactive microstate (those identified with an asterisk in *Fig.*1) in k steps, visiting only reactive states in the previous $k-1$ steps, therefore,

$$U(k) = \sum_{j*} e_{j*k} \tag{10}$$

where the summation is restricted to nonreactive microstates. *Figure 3* schematically shows how $U(k)$ is constructed.

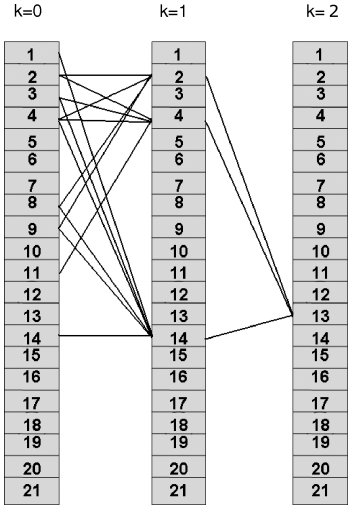

Figure 3: Transitions to evaluate e_{13^*2}, the probability of arriving at the nonreactive microstate 13^* in $k = 2$ steps without starting from $(k = 0)$ or previously visiting $(k = 1)$ nonreactive states (see *Eq.* 10).

Let $< t >$ be the average number of steps necessary to deactivate the lattice first, therefore,

$$< t >= \sum_{k=0}^{\infty} kU(k) \tag{11}$$

where $< t >$ is equivalent to the number of Monte Carlo steps in a simulation.

Let σ be the standard deviation of $< t >$, then

$$\sigma = \sum_{k=0}^{\infty} (k - < t >)^2 U(k) \tag{12}$$

Note that $< t >$, as defined by *Eq.* 11, *is the average number of reactive states necessary to deactivate the lattice first. As the reaction considers desorption processes, it does not stop after this type of event and, therefore, the concentration of products fluctuates over time. Besides,* $< t >$ is independent of the initial distribution of microstates and then is the average time of fluctuations. Thus, $< t >$ is a characteristic time of the reaction and its determination may be important when a constant flow of products is required

3 Results and Conclusions

The average deactivation time ($< t >$) was determined from *Eq.* 11 starting with several sets of initial distribution of microstates, and no significant differences were found. To further investigate the reason for that independence, we determined what particular microstates are created starting from every microstate. We found that the set of 21 microstates shown in *Fig.* 1 can be divided into two sets. One of them (*Set A*) is formed by microstates $1, 12$ *and* 18, and the other (*Set B*), by the remaining microstates. From any element of *Set A* the 21 microstates ($A \cup B$) can be generated in a few steps, whereas starting from any element of *Set B* only the elements of *Set B* are generated. The reason for this division lies in the transition matrix probability. When the control parameters s and p_d are different from 0 or 1,

$$P_{ij} \neq 0, \ i \in A, \ j \in B \tag{13}$$

and

$$P_{ji} = 0, \ i \in A, \ j \in B \tag{14}$$

Therefore, when the number of steps $k \to \infty$, we come to the following conclusion:

$$\lim_{k \to \infty} \ e_{ik} = 0, \ i \in A \tag{15}$$

and

$$\lim_{k \to \infty} \ e_{jk} = e_{j\infty} \neq 0, \ j \in B \tag{16}$$

After overcoming a transient and independently of starting from *any individual microstate* or from a *set of microstates,* when the number of steps $k \to \infty$, we arrive at a

unique final probability distribution of microstates,

$$e_{j\infty} = f(s, p_d),\ j \in B \tag{17}$$

$$e_{i\infty} = 0,\ i \in A \tag{18}$$

depending only on the control parameter (s and p_d) values employed in the transition matrix probability, and independently of the initial probability distribution used.

These conclusions explain why $< t >$is independent of the initial probability distribution of microstates.

Figure 4*a* shows the dependence of $< t >$ on p_d at different s values, whereas *Fig.* 4*b* shows the dependence of $< t >$ on s at different p_d values.

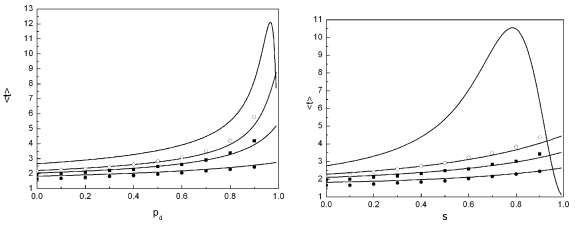

(a) (b)

Figure 4: *(a)* Dependence of $< t >$ on p_d at different values of s on a 2×2 lattice. From bottom to top $s = 0, 0.5, 0.7, 1.0$. *(b)* Dependence of $< t >$ on s at different values of p_d on a 2×2 lattice. From bottom to top $p_d = 0, 0.5, 0.7, 1.0$. Lines and symbols indicate analytical and Monte Carlo simulation results, respectively.

Monte Carlo simulations were used to study the reaction characteristics on larger lattices. Values of $k_d = 10^{13} s^{-1} exp\left[-\frac{109 KJ/mol}{RT}\right]$, $k_r = 10^9 s^{-1} exp\left[-\frac{62.1 KJ/mol}{RT}\right]$(where R is the gas constant and $350 < T < 800$) and $k_a = 2.22 \times 10^5 mbar^{-1} s^{-1}$were used in the simulations. Also, $k_d = 0$ (and therefore $p_d = 0$) were used for comparison. At $T = 500K$, all the parameters take the values given in Section 2.

Figure 5 shows simulations performed on 4×4 and 8×8 lattices. In both cases a pattern similar to that observed on a 2×2 lattice is obtained, though $< t >$ reaches a maximum value at lower s and p_d values. On small lattices the adsorption and desorption processes must dominate the reaction dynamic to reach nonreactive microstates. As the lattice size increases also increases the number of microstates and the reaction process becomes more dominant in the reaction dynamics. Computation times in Monte Carlo simulations increase with N and p_d. For this reason p_d values close to one were not

included in *Fig.* 5. The different p_d values were included to show the nonmonotonic behavior of $< t >$ on s and p_d, at different lattice sizes (N).

Despite the reduced number of sites employed, the analytical solution shows the general features observed by simulating the mechanism on a large $N \times N$ lattice. Indeed, the main differences are (i) the dependence of $< t >_{\max}$ on s and p_d, which is polynomial, and (ii) the dependence of $< t >$ on N. The study of both of them requires simulations with large N values and will be treated in a forthcoming paper.

While analytical calculation (and simulations on small lattices) demands only a few seconds, on PCs Core2QuadQ6600, simulations on 8×8 lattices can demand a couple of months on the same hardware depending on the s and p_d values.

In table 1 we compare typical real computation times (for one independent run) in lattices of different sizes.$< t >$ was calculated by averaging on about 2000 independent runs.

Lattice size	s;pd values	Average real computation time (sec.)
2×2	0.6 ; 0.9	9×10^{-3}(calculated)
4×4	0.6 ; 0.9	0.22 (calculated)
8×8	0.6 ; 0.9	2520 (measured)

Table 1: Comparison of real times for the computation of deactivation time on different lattice sizes.

This result should encourage the search for an analytical solution as a reliable form to unravel details of a chemical reaction prior to performing time-consuming numerical simulations on large lattices.

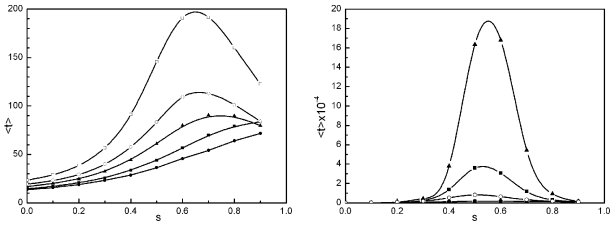

(a) (b)

Figure 5: Dependence of $< t >$ on s at different values of p_d. Monte Carlo simulations performed on a 4×4 lattice and $p_d = 0.0, 0.1, 0.5, 0.7, 0.9$ (from bottom to top) *(a)*, and an 8×8 lattice and $p_d = 0.5, 0.7, 0.8, 0.9$ (from bottom to top) *(b)*.

Acknowledgements: This work was financially supported by the Consejo Nacional de Investigaciones Científicas y Técnicas CONICET, Universidad Nacional de La Plata UNLP, and Agencia Nacional de Promoción Científica y Tecnológica ANPCyT.

References

[1] J. P. L. Segers, *Algorithms for the Simulation of Surface Processes*, Technische Univ. Eindhoven, Eindhoven, 1999.

[2] A. P. J. Jansen, *An Introduction to Kinetic Monte Carlo Simulations of Surface Reactions*, Springer, Berlin, 2012.

[3] E. A. Kotomin, V. N. Kuzovkov, *Modern Aspects of Diffusion–Controlled Reactions: Cooperative Phenomena in Bimolecular Processes*, Elsevier, Amsterdam, 1996.

[4] P. Érdi, J. Tóth, *Mathematical Models of Chemical Reactions – Theory and Applications of Deterministic and Stochastic Models*, Princeton Univ. Press, Princeton, 1989.

[5] A. V. Zhdanova, Simulation of the kinetics of rapid catalytic reactions on ultrasmall metal particles, *Phys. Rev. B* **63** (2001) 153410.

[6] V. P. Zhdanov, B. Kasemo, Simulations of the reaction kinetics on nanometer supported catalyst particles, *Surf. Sci. Rep.* **39** (200) 25–104.

[7] A. E. Bea, A. V. Ranea, I. M. Irurzun, E. E. Mola, Kinetics of immobile adsorption of linear molecules on a two–dimensional lattice, *Chem. Phys. Lett.* **401** (2005) 342–346.

[8] A. E. Bea, I. M. Irurzun, E. E. Mola, How many Langmuirs are required for monolayer formation? *Langmuir* **21** (2005) 10871–10873.

[9] I. M. Irurzun, V. A. Ranea, E. E. Mola, Branch counting probability approach to random sequential adsorption, *Chem. Phys. Lett.* **408** (2005) 19–24.

[10] A. E. Bea, I. M. Irurzun, E. E. Mola, Scaling properties in the average number of attempts until saturation in random sequential adsorption processes, *Phys. Rev. E* **73** (2006) 051604.

[11] P. Bergero, V. Pastor, I. M. Irurzun, E. E. Mola, The heterogeneous catalytic reaction $2A + B_2 \rightarrow 2AB$ exactly solved on a small lattice, *Chem. Phys. Lett.* **449** (2007) 115-119.

[12] P. L. Dammig Quiña, V. E. Pastor, I. M. Irurzun, E. E. Mola, Configurational degeneracy of a set of dipoles in a quasi–two–dimensional system, *J. Math. Chem.* **48** (2010) 592–600.

[13] M. Gruyters, T. Ali, D. A. King, Theoretical inquiry into the microscopic origins of the oscillatory CO oxidation reaction on Pt{100}, *J. Phys. Chem.* **100** (1996) 14417–14423.